Optimization of the FeCo nanowire fabrication embedded in anodic aluminum oxide template by response surface methodology

Mi. Salehi [1], P. Marashi [1], Ma. Salehi [2], R. Ghannad[1]

Abstract

Anodic aluminum oxide (AAO) fabricated by two step anodization technique, is used as a template to synthesize FeCo nanowire arrays by AC electrodeposition technique. Response surface methodology (RSM) is applied to design the experiments, fit an empirical model and optimize the conditions to achieve the best magnetic properties. The magnetic properties, pore dimensions, composition and structure of the nanowires are characterized through alternating gradient force magnetometer (AGFM), scanning electron microscopy (SEM), scanning probe microscopy (SPM), energy dispersive spectoroscopy (EDS) and X-ray diffraction (XRD), respectively. The effects of annealing temperature (T_a), Fe concentration (C), the pH of the deposition solution (pH) and electrodeposition temperature (T_d) on the magnetic properties are investigated. Maximum experimental coercivity field (H_c = 191.4 KA/m) is obtained in the following conditions: T_a = 550 °C; C = 50 wt%; pH = 6; T_d = 40 °C. The optimum values to obtain maximum predicted coercivity field (H_c = 195.5 KA/m) are predicted with a statistical technique as: T_a = 575 °C; C = 50.3 wt%; pH = 6; T_d = 39 °C. Moreover, the results show that T_d^2 and T_a are the most important parameters affecting coercivity field. XRD results show that the crystal structure of nanowires is BCC with (1 1 0) preferred orientation along the nanowire axis.

Keywords: Nanowires; Electrodeposition; Anodic aluminum oxide; Coercivity field; Response surface methodology

1. Introduction

Recently, much interest has been devoted to fabricate FeCo nanowires due to their application in magnetic sensors and perpendicular magnetic recording devices. A material used in magnetic recording should exhibit high anisotropy and relatively large coercivity (H_c) and squareness (M_r / M_s) [1-6]. Among the current fabrication methods, electrodeposition in porous materials such as anodized aluminum is one of the most promising technologies to prepare nanowires with high perpendicular magnetic anisotropy. Porous aluminum oxide (PAO) templates are easily fabricated and have the advantage of high pore densities and also very uniform and nearly parallel pores organized in a hexagonal close packed array [1-3,5,7-8]. FeCo nanowires electrodeposited into AAO templates have been studied by many research groups [1-7]. In contrast to Fe, Co or Ni, the FeCo alloy has high saturation magnetization, low crystalline anisotropy (K_1) and high Curie temperature, presenting appropriate parameters for high temperature applications [1, 3].

The aim of our study is to investigate the influence of process parameters on the magnetic properties and optimize the conditions to achieve the highest coercivity field in the FeCo nanowires by response surface methodology (RSM). RSM is a combination of mathematical and statistical techniques to fit an empirical model of process and obtain the optimum operating conditions for the involved parameters, where a desired response is influenced by several variables. The other objective of RSM is to determine a region of the factor space in which operating requirements are satisfied [9-10]. The independent variables examined included annealing and electrodeposition temperatures,

1- Department of Mining and Metallurgical Engineering, Amirkabir University of Technology, Tehran, Iran.
2- Center of Excellence for High Strength Alloys Technology (CEHSAT), School of Metallurgy and Materials Engineering, Iran University of Science and Technology (IUST), Tehran, Iran.

Corresponding author: M. Salehi, Department of Mining and Metallurgical Engineering, Amirkabir University of Technology, Tehran, Iran.
Email: m_salehi1389@yahoo.com

Fe concentration and pH of deposition solution.

2. Experimental

The pure aluminum (99.95%, Merck) plate was cut into circular pieces with 13 cm diameter. The samples were degreased in acetone for 1 h and annealed at 450 °C for 15 min, then were etched in 0.3 M NaOH for 3 min. Subsequently **t**he samples were electropolished at 400 mA in a 1:4 volume mixture of HClO4 and C2H5OH at room temperature. To obtain highly ordered pores, a two-step anodization process was employed. The first anodization was carried out at a constant voltage of 40 V in 0.3 M oxalic acid at 17 °C for 15 h. Afterwards, in STP process all samples were rinsed in a 0.5 M H3PO4 and 0.2 M H2CrO4 aqueous solution at 60 °C for 6 h. The samples were re-anodized for 1 h using the same conditions as in the first step. Following the second anodization, for thinning the barrier layer the voltage was systematically reduced to 20 V by 4 Vmin-1, then to 10 V by 2 Vmin-1 and finally to 8 V in an interval of 1 Vmin-1. The anodization was performed for 3 min at this final voltage to equilibrate the barrier layer and uniform it's thickness at the bottom of the pores.

The magnetic properties were studied at room temperature by an alternating gradient force magnetometer. The hysteresis loops were drawn with magnetic field parallel to the wire axis. The AAO film was perceived by means of a Philips-XL30 scanning electron microscopy and a DME model, serial DS95 scanning probe microscopy. X-ray diffraction (X-Pert-Pro 2001) and the SEM attached with energy dispersive spectroscopy were used to analyze the crystalline structure and the composition of nanowires, respectively.

2.1. Experimental design

The FeCo nanowires were electrodeposited with an electrolyte containing $CoSO_4.7H_2O$, $FeSO_4.7H_2O$ and 45 gl^{-1} boric acid, while the solution was continuously agitated by a magnetic stirrer. The AC electrodeposition was performed using a sine wave form with voltage and frequency of 30 V_{p-p} and 1000 Hz, respectively. The reductive and oxidative voltages were -15 V and 15 V, respectively, while the deposition time was 90 s for all samples. At the final step, the samples were annealed at different temperatures (525 °C, 550 °C, 575 °C and 600 °C) in Ar atmosphere with low vacuum pressure of 10^2 Pa for 2 h, then slowly cooled down to room temperature.

The applied optimization approach to achieve the maximum coercivity field is based on response surface methodology and the experiments were designed using D-optimal criterion. The D-optimal design allows selecting the points to minimize the variances of the model regression coefficients. A non-optimal design requires a larger number of experiments to estimate the parameters with the same precision as an optimal design [9-11].

In the present study, the independent variables of annealing temperature, Fe concentration, pH of deposition solution and the electrodeposition temperature are coded with low and high levels in D-optimal design, while the coercivity field of the nanowires is the response. The coded values ($x_{j,i}$ = 1, 2, 3, 4) and parameter levels (α = -2, -1, 0, 1, 2) are listed in Table 1. Therefore, 15 experiments are considered on the basis of D-

Table 1. Parameter levels and coded values used in the experimental design

Parameter	Code	α = +2	α = +1	α = 0	α = -1	α = -2
T_a (°C)	X_1	600	575	550	525	
T_d (°C)	X_2	60	50	40	30	20
pH	X_3	6	5	4	3	2
C (wt%)	X_4	70	60	50	40	30

optimal design. The analysis of the experimental data is carried out by multiple regressions to fit the second order polynomial equation to all independent variables. A quadratic model, which also includes the linear model, is described by Eq. (1) [9-12].

$$Y = a_0 + \sum a_i . X_i + \sum a_{ii} . X_i^2 + \sum a_{ij} . X_i . X_j \qquad (1)$$

where Y represents the response, a_0 is a constant, a_i, a_{ii} and a_{ij} are the linear, quadratic and interactive coefficients, respectively; X_i and X_j are coded experimental levels of the variables. Variance analysis was performed to test the significance and adequacy of the model. A systematic method is proposed for optimizing the conditions to achieve the best performance of magnetic nanowires. To portray the relationships between the responses and the independent variables, contour plots of the fitted regression model were generated.

3. Result and Discussion

The magnetic hysteresis loop of $Fe_{51}Co_{49}$ nanowire is shown in Fig. 1. The H_c with external field parallel to the nanowire arrays from all the experiments are given in Table 2. In addition, the experimental data is used to predict the values of H_c (Table 2). So, the H_c of the nanowires can be estimated with the following equation [9-12]:

$$H_c = -36009.3 + 133.518\,T_a - 469.631\,pH + 24.0798\,T_d + 38.0196\,C - 0.129937\,T_a^2 - 19.9606\,pH^2 - 1.38298\,T_d^2 - 0.378322\,C^2 + 1.48385\,T_a \times pH + 0.179883\,T_a \times T_d - 3.22324\,pH \times T_d \qquad (2)$$

where H_c is the coercivity field, T_a, C, pH and T_d are annealing temperature, Fe concentration percentage, pH of deposition solution and electrodeposition temperature, respectively. The units of temperatures and coercivity field in this equation are degree centigrade (°C) and oersted (Oe), respectively.

Because of various kinds of imperfection in the wire and the influence of magnetostatic interactions between wires, a**n** actual magnetic nanowire is far more complicated than a collection of impendent particles according to Stoner and Wohlfarth model. This approach significantly overestimates the coercivity of the wires. Recently, localized nucleation mode has been proposed by Skomski et al. which is in view of polycrystalline structure of the wires and magnetization perturbances associated with wire-thickness fluctuations, crystalline

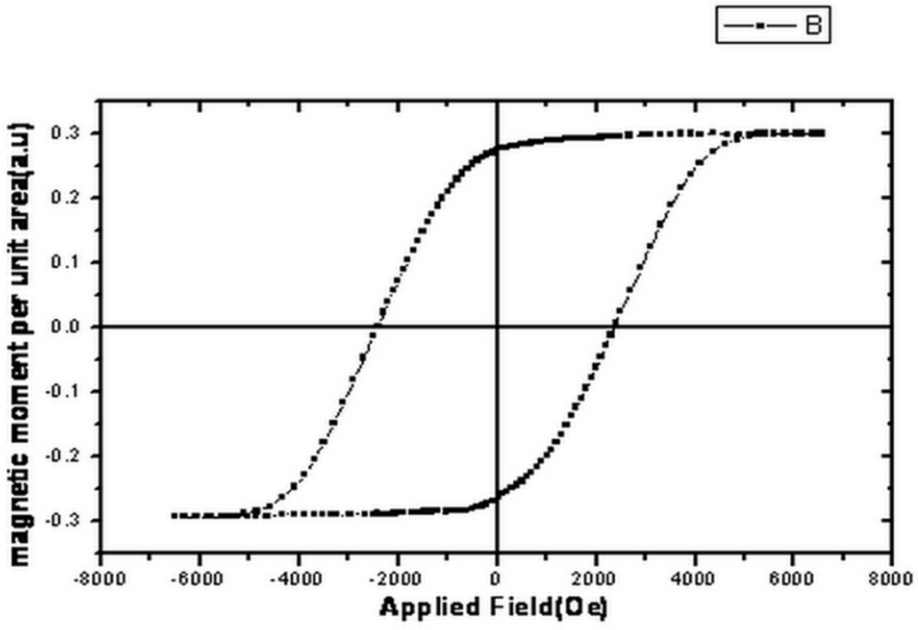

Fig. 1. Hystersis loop of $Fe_{59}Co_{41}$nanowire

Table 2. Design layout with actual and predicted responses for D-optimal design

Experimental number	T_a (°C)	(°C) T_d	pH	C (wt% Fe)	H_c (Oe – (KA/m)) Experimental	Predicted
1	550	20	4	50	1794.67 (142.8)	1790.77 (142.5)
2	525	30	3	40	1997.17 (158.9)	1958.63 (155.9)
3	525	30	5	60	2025.96 (161.2)	2068.39 (164.6)
4	575	30	5	60	2241.19 (178.3)	2238.54 (178.1)
5	550	40	2	50	2095.63 (166.8)	2138.06 (170.1)
6	550	40	4	50	2333.64 (185.7)	2333.64 (185.7)
7	600	40	4	50	2188.20 (174.1)	2194.72 (174.6)
8	550	40	4	30	2175.30 (173.1)	2178.57 (173.4)
9	550	40	4	70	2182.80 (173.7)	2186.06 (174.0)
10	550	40	6	50	2405.45 (191.4)	2369.54 (188.6)
11	525	50	3	60	1930.48 (153.6)	1926.58 (153.3)
12	575	50	3	60	2177.21 (173.3)	2128.25 (169.4)
13	525	50	5	40	1906.44 (151.7)	1899.92 (151.2)
14	575	50	5	40	2217.96 (176.5)	2249.97 (179.0)
15	550	60	4	50	1759.71 (140.0)	1770.13 (140.9)

defects, impurities and geometrical features at the wire ends. The localization of the nucleation mode is accompanied by a coercivity reduction. Based on the research of Skomski et al., the corresponding coercivity could be expressed as follows:

$$H_C = 2\frac{K_{eff}}{\mu_0}M_S - \frac{\alpha^2\Delta K^2}{2\,A\,\mu_0 M_S} = \frac{\mu_0 M_S}{2} - \frac{\alpha^2\Delta K^2}{2\,A\,\mu_0 M_S} \quad (3)$$

where H_C is coercivity field, K_{eff} is effective uniaxial anisotropy determined by magnetocrystalline anisotropy and shape anisotropy, μ_0 is permeability of vacuum, α is the length which determines the defect's volume, M_s is saturation magnetization, ΔK is the reduced local anisotropy via the localization length accompanied by an easy-axis misalignment and A is the exchange stiffness. By means of the formula one can rationalize H_c values of 20% - 30% of H_A (anisotropy field, $H_A = \mu_0 M_s /2$), as often observed. In the case of FeCo, M_s is about 1.5 - 2.4 T. So H_c is estimated to be about 1800 - 3800 Oe. In our study H_c is in the range of 1760 - 2405 Oe, showing good agreement with localized nucleation mode, the same as results have been obtained in Lin Cao et al. work [13]. So the localized reversal model is appropriate

to explain the reversal process in our FeCo nanowires.

The multiple regression results and the significance of regression coefficients for this model are listed in the Table 3. The significant parameters are specified based on the T and P-values. The P-value is useful to check the significance of each coefficient, which in turn is necessary to understand the pattern of mutual interactions between the variables. The corresponding coefficient with a low P-value ($P < 0.05$) and a high absolute T-value, is extremely significant [12]. Therefore, two parameters with the most important effect on the H_c are T_d^2 and T_a, respectively. The Fe concentration has the least effect on the H_c. The quality of the fitting of the second order equation can be expressed by the regression coefficient (R^2) [11]:

$$R^2 = 1 - \frac{SS_{residual}}{SS_{model} + SS_{residual}} \qquad (4)$$

where SS is sum of squares for each variation sources. The R^2 value (0.9799) is acceptable and shows a good agreement with the experimental and predicted values of the model. Variance analysis for the quadratic model is presented in Table 4. This statistical tool is required to test the significance and adequacy of the model. The mean squares (MS) are obtained as follows [12]:

$$MS = \frac{SS}{DF} \qquad (5)$$

where DF is the respective degrees of freedom. The Fischer variation ratio (F-value) is a measure that shows how well the factors describing the variation of data around its mean value. It can be calculated as follows [12]:

$$F - value = \frac{MS\ (duetothemodelvariation)}{MS\ (duetoerrorvariance)} \qquad (6)$$

The larger F-value from unity explains adequately the variation of the data around its mean and that the estimated factor effects are real. The results show that the quadratic polynomial model is qualified to describe the influence of independent variables on the response. The calculated F-value which corresponds to response model is 13.27 that exceeds the tabulated F-value for the model ($F_{0.05}$ (11,3) = 8.765) at the 5% level, demonstrating that the model is suitable (Table 4) [12]. The P-value is relatively low, showing the significance of the model. Fig. 2 illustrates actual values of H_c against predicted amount of the regression model. From this figure, existence of high linearity between actual and predicted values prove the accuracy of model.

The optimum values of variables to obtain maximum H_c can be predicted with a statistical technique which is listed in Table 5. According to this table, the optimum values to obtain

Table 3. Terms of quadratic model with their Coefficients and significance indices (R^2 = 0.9799)

Term	T	P
T_d^2	-7.895	0.004
T_a	4.394	0.022
T_a^2	-3.918	0.030
pH	3.694	0.034
C^2	-2.160	0.120
$T_a \times T_d$	1.895	0.154
$T_a \times pH$	1.563	0.216
pH^2	-1.140	0.337
$pH \times T_d$	-1.029	0.379
T_d	-0.329	0.764
C	0.092	0.933

Table 4. Variance analysis for the quadratic model

Source	DF	SS	MS	F	P
Regression	11	488947	44449.7	13.27	0.028
Linear	4	130160	32540.0	9.71	0.046
Square	4	332664	83166.0	24.83	0.012
Interaction	3	17062	5687.4	1.70	0.337
Residual Error	3	10050	3350.0	-	-
Total	14	-	-	-	-

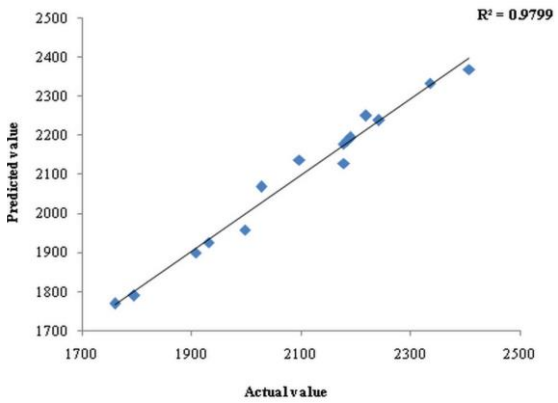

Fig. 2. Actual and predicted plot for the coercivity field of the nanowires (R^2 = 0.9799)

maximum predicted H_c (195.5 KA/m) are extracted as: T_a = 575 °C; C = 50.3 wt%; pH = 6; T_d = 39 °C, while maximum experimental H_c (191.4 KA/m) is obtained in the following conditions: T_a = 550 °C; C = 50 wt%; pH = 6; T_d = 40 °C.

To visualize the effect of the independent variables on the H_c, contour plots of the quadratic polynomial model are generated by varying two selected variables within the experimental range, while holding the other two constant at the central point (Fig. 3). According to Fig. 3 (a,b,c), the H_c increases with annealing temperature and reaches its maximum value at 575 °C, then decreases up to 600 °C. The increase of H_c with increasing T_a up to 575 °C can be justified by two important factors. First, after annealing the internal stress in deposited sample is reduced and a higher degree of crystallinity and also higher M_s and is H_c obtained. Second, there is a large mismatch between the thermal expansion coefficients (α) of FeCo alloy and alumina. At room temperature α_{Co} is about 14.0×10^{-6} K^{-1}, while α_{AAO} is about 6.0×10^{-6} K^{-1}. FeCo alloy prefers to expand freely along the wire axis during annealing and form column structure with easy axis along nanowire arrays. Therefore, the mismatch of α can increase the external anisotropy along the

Table 5. Optimum values of variables to obtain maximum H_c

variable	T_a (°C)	T_d (°C)	pH	C (wt% Fe)
Critical value	575	39	6	50

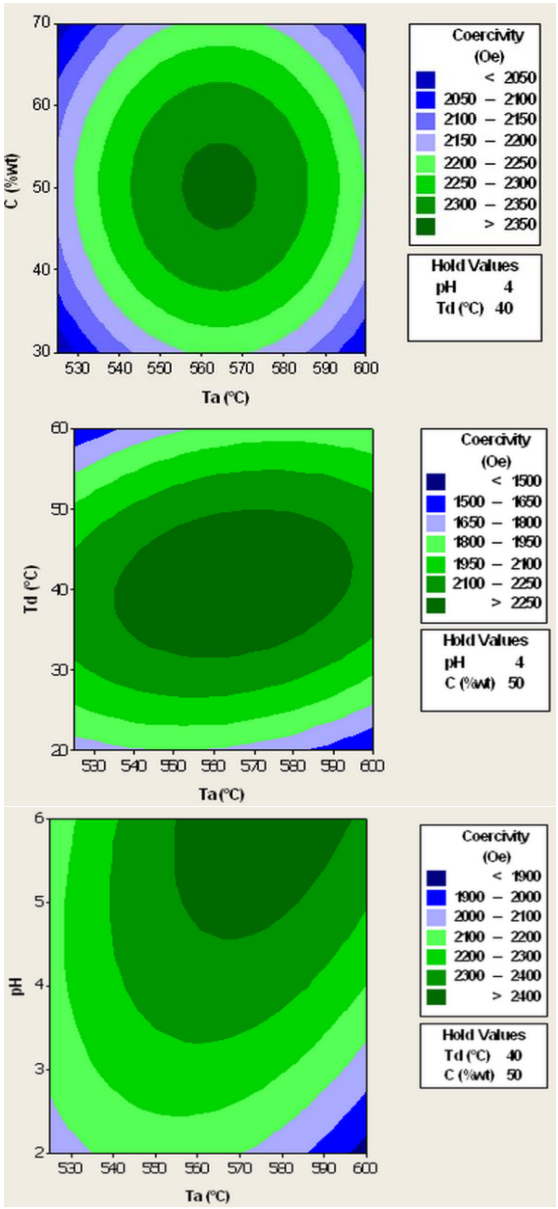

Fig. 3. Contour plots showing the effects of experimental factors on the coercivity field of the nanowires (a) C and T_a on the H_c when pH and T_d were 4 and 40 °C, respectively; (b) T_d and T_a on the H_c when C and pH were 50 wt% and 4, respectively (c) pH and T_a on the H_c when T_d and C were 40 °C and 50 wt%, respectively

wire axis when the samples are heat treated, which enhance the H_c of the nanowires [1,3,5,13].

For the annealing temperature higher than 575 °C, internal stress will distort the alumina and deviates the pores from its original place, which will decrease the shape anisotropy and H_c [1]. In addition, at high temperature FeCo can react with O_2 exist in AAO template and

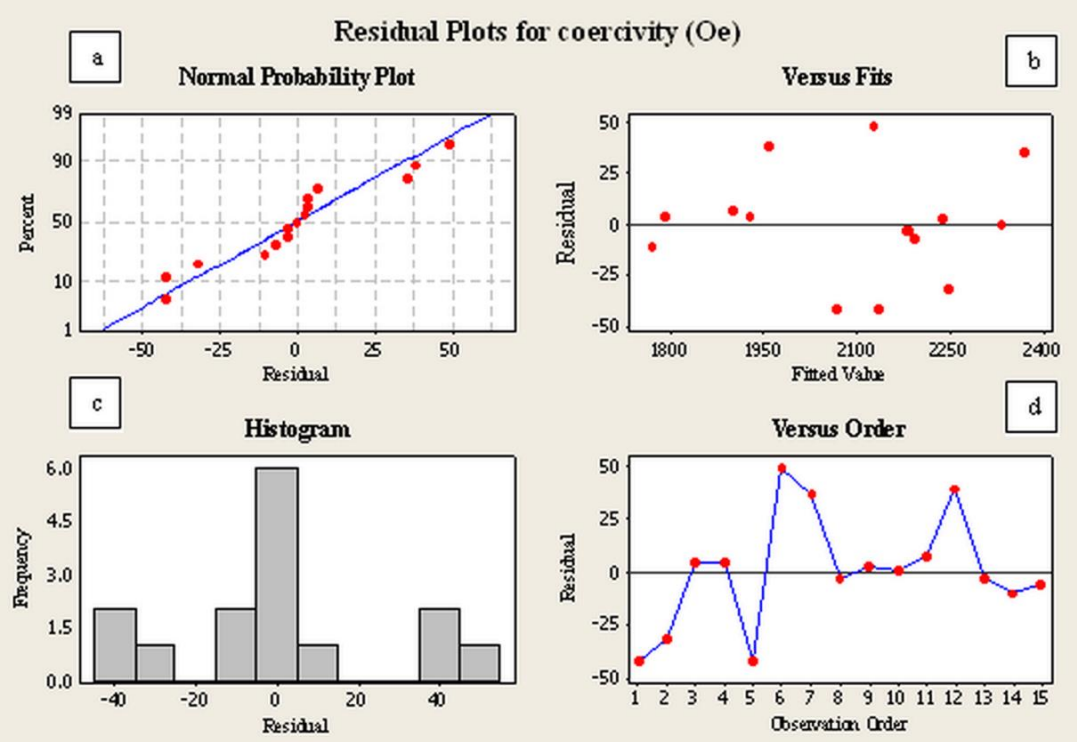

Fig. 4. Residual analysis for the response surface regression of the data: (a) normal probability plot of the residuals, (b) residuals versus the fitted values, (c) histogram of the residuals, (d) residuals versus the order of the data

presence of FeCo oxide will decrease the M_s extremely in the samples. These two factors will reduce the anisotropy along the axis of FeCo arrays [1,13].

The results of residual analysis for the response surface regression of the data are shown in Fig. 4. Fig. 4 (a) shows the normal probability plot of residuals. If the residuals plot is approximately along a straight line, the normality assumption is satisfied. In this study, the residuals can be judged as normally distributed. Therefore, normality assumption for the H_c is satisfied. Fig. 4 (b) shows the residuals versus predicted values. This plot is a random scatter, showing that the variance of original observations is constant for all values of the response. Fig. 4 (c) displays the histogram of residuals, which is a graphical technique that shows the distribution of the residuals for all observations and for assessing whether or not the data set is approximately normally distributed. According to this figure, a typical bell-shaped histogram with low skewness (lack of symmetry) is obtained. Fig. 4 (d) shows the residuals versus the order of the data which is used to check how the order of experimental runs can affect the data. In the current case, the residuals are found to fluctuate in a random pattern around the center line of Fig. 4 (d), which indicate the level of randomization is suitable and that the order of testing has no effect on the data [14].

Fig. 5 shows the typical SPM and SEM results of AAO template. According to Fig. 5 (a,b) the average diameter and length of pores in AAO template are about 30 nm and 6 μm, respectively. The results of EDS analysis for sample 14 is shown in Table 6, which demonstrates that the atomic ratio of Fe to Co is close to 4:6. As the radius of hydrated ions of Fe^{2+} and Co^{2+} are almost equivalent, the migratory velocity of Fe^{2+} is almost the same as that of Co^{2+}. Studies show that the electrodeposition velocity of Fe^{2+} or Co^{2+} is strongly controlled by the migration velocity of Fe^{2+} or Co^{2+}, which is related to the radius of ions. Therefore, the compositions of nanowires are controlled by the relative ratio of Fe^{2+} and Co^{2+} [13].

The XRD spectra of $Fe_{66}Co_{34}$ nanowire is shown in Fig. 6. From this figure, the main diffraction peak can be assigned to FeCo (1 1

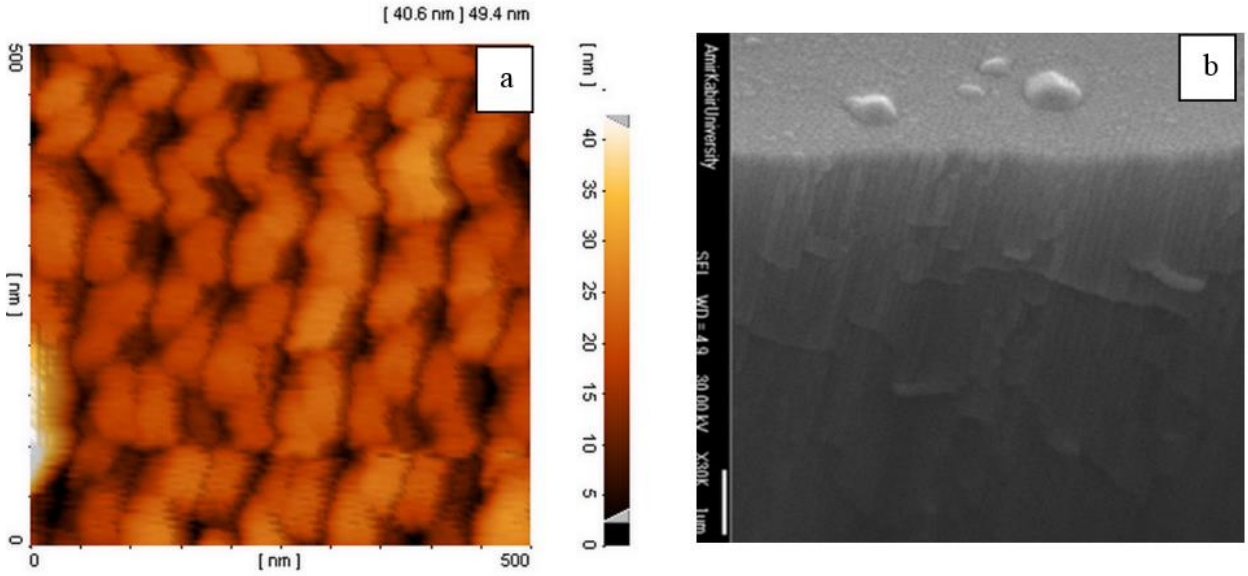

Fig. 5. (a) AFM and (b) SEM image of AAO template

Table 6. The EDS results of sample 14

Element	Line	wt%	K-ratio	at%
Fe	Ka	40.89	0.4190	42.20
Co	Ka	59.11	0.5871	57.80

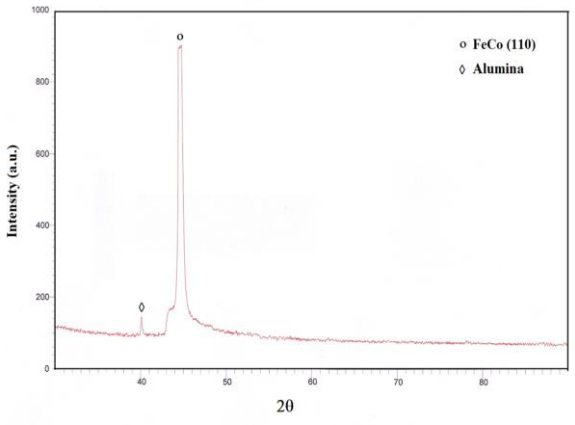

Fig. 6. XRD spectra of $Fe_{66}Co_{34}$ nanowire

0), which indicates that the nanowire is a BCC structure with (1 1 0) preferred orientation along the nanowire axis. The other peak (2H = 40) can be assigned to the peaks of alumina [1-3,5-6,13]. According to the EDS results, the Fe content in the samples is in the range of 27 - 68 at% and BCC - FeCo (1 1 0) is identified. Whereas in similar works with 10 - 27 at% Fe, the graph also shows a FCC - Co (1 1 1) peak besides BCC - FeCo (1 1 0) structure. This means that the FeCo nanowires undergo a phase transformation from α (BCC - FeCo) to γ (BCC - FeCo and FCC - Co) by increasing the Co content [13].

4. Conclusions

Response surface methodology with a D-optimal design has been used to investigate the effect of process factors on the magnetic properties of FeCo nanowires embedded in AAO template. The results show that the second-order polynomial model is sufficient to predict the response of the coercivity field. The regression coefficient R^2 (0.9799) and the F-test within the experimental range prove the validity of polynomial model. T_d^2 and T_a are the most important parameters affecting H_c. By using graphical method the process factors to achieve the highest H_c (195.5 KA/m) are extracted as follows: T_a = 575 °C; C = 50.3 wt%; pH = 6; T_d = 39 °C. XRD spectra shows that the nanowires are BCC structure with (1 1 0) preferred orientation along the nanowire axis.

Acknowledgements

The authors would like to have special thanks to Department of Mining and Metallurgical Engineering of Amirkabir University of Technology. The authors are also thankful for the financial support of the Iran nanotechnology initiative council.

References

1. Qin, D. H., Peng. Y., Cao. L., Li, H. L., *Chem. Phys. Lett.* Vol 374 (2003) pp. 661-6.
2. Tang, S. L., Chen, W., Lu, M., Yang, S. G., Zhang, F. M., Du, Y. W., *Chem. Phys. Lett.* Vol 384 (2004) pp. 1-4.
3. Guo, Y., Qin, D. H., Ding, J. B., Li, H. L., *Appl. Surf. Sci.* Vol 218 (2003) pp. 106-12.
4. Saedi, A., Ghorbani, M., Mater. *Chem. Phys*.Vol 91 (2005) pp. 417-23.
5. Qin, D. H., Cao, L., Sun, Q. Y., Huang, Y., Li, H. L., *Chem. Phys. Lett.* Vol 358 (2002) pp. 484-8.
6. Gao, J., Zhan, Q., He, W., Sun, D., Cheng, Z., *J. Magn. Magn. Mater*. Vol 305 (2006) pp. 365-71.
7. Zhixun, L., Yan, F., Xiaofang, Z., Jiannian, Y., *Mater. Chem. Phys.* Vol 107 (2008) pp. 91-5.
8. Gerein, N. J., Haber, J. A., J. Phys. *Chem. B.* Vol 109 (37) (2005) pp. 17372-85.
9. Montgomery, D. C., Design and analysis of experiments, fifth ed. (2001) pp. 427-510, John Wiley & Sons Inc.
10. Hinkelmann, K., kempthorne, O., Design and analysis of experiments: Introduction to experimental design, Vol 1, second ed. (2008) pp. 497-531, John Wiley & Sons Inc.
11. Körbahti, B. K., Rauf, M. A., *Chem. Eng. J.* Vol 136 (2008) pp. 25-30.
12. Hamzaoui, A. H., Jamoussi, B., Mńif, A., *Hydrometallurgy.* Vol 90 (2008) pp. 1-7.
13. L ,Cao., Qiu, X., Ding, J., Li, H., Chen, L., *J. Mater. Sci.* Vol 41(2006) pp. 2211–18.
14. Küngas, R., Kivi, I., Lust, K., Nurk, G., Lust, E., *J. Electroanal. Chem.* Vol 629 (2009) pp. 94-101.